# Blind frequency offset estimation based on cyclic prefix and virtual subcarriers in CO-OFDM system

**Yaojun Qiao (乔耀军)*, Zhansheng Wang (王战胜), and Yuefeng Ji (纪越峰)**

*Key Laboratory of Information Photonics and Optical Communications (IPOC), Ministry of Education (MOE), Beijing University of Posts and Telecommunications, Beijing 100876, China*

**E-mail: qiao@bupt.edu.cn*

Received June 1, 2010

A new blind frequency offset estimation method based on cyclic prefix and virtual subcarriers in coherent optical orthogonal frequency division multiplexing (CO-OFDM) system is presented. It is able to estimate the fractional part and integral part of frequency offset at the same time. Its estimation range is about [−3.5 GHz, 3.5 GHz]. The influence of the integral frequency offset is comprehensively analyzed in CO-OFDM system. Its performances in the additive white Gaussian noise (AWGN) channel and the dispersive channel are investigated, respectively. Simulation results indicate that even in the dispersive channel, when the optical signal-to-noise ratio (OSNR) is low, it can still work very well.

*OCIS codes:* 060.0060, 060.1660, 060.2330, 060.5060.

*doi: 10.3788/COL20100809.0888.*

Ultra high speed and high level modulation have become hot topics of investigation in optical communication[1−3]. Orthogonal frequency division multiplexing (OFDM) technique is an effective transmission scheme to cope with many channel impairments, such as chromatic dispersion (CD) and polarization mode dispersion (PMD). It has recently gained increasing interest in optical communication[4,5]. Nowadays, coherent optical OFDM (CO-OFDM) is a promising scheme for high speed optical transmission. However, one of the well known problems in CO-OFDM is its sensitivity to synchronization errors, including frequency offset. All of the subcarriers in OFDM system are overlapped and orthogonal to each other, so a minor carrier frequency offset will make these subcarriers lose their orthogonality[6]. Frequency offset significantly degrades system performance and causes inter-carrier interference (ICI). For this reason, the estimation of carrier frequency offset is a crucial task in OFDM systems.

In general, frequency offset estimation algorithms can be classified into two folds based on whether the additional data are used or not. Training symbols and pilot subcarriers are two kinds of redundancy data which are employed. Training symbols have been exploited to estimate frequency offset[7]. The method utilizing pilots to estimate frequency offset has also been proposed[8]. The shortcoming of data-aided methods is the loss of bandwidth efficiency.

One of the major advantages in OFDM is that it can eliminate inter-symbol interference (ISI) due to cyclic prefix (CP). CP is inserted to the head of each OFDM symbol before transmission, which is the copy of signals in the end of the OFDM symbol[9]. Therefore, CP is a kind of redundant information. The blind methods rely on the nature structure of OFDM symbols to estimate the frequency offset. In this scenario, synchronization can be done at every OFDM, so it is very suitable for the CO-OFDM system. A maximum likelihood (ML) frequency offset estimation based on CP was introduced in Ref. [10]. This method exploits the cyclostationarity properties of OFDM symbols because of the insertion of CP. However, the frequency offset estimation method based on CP is only used to estimate the fractional frequency offset. There are many methods for integral frequency offset estimation. The method proposed in Ref. [7] uses differential information between two consecutive blocks of OFDM symbols to estimate the integral frequency offset, which is an integer multiple of the subcarrier spacing. Another method was presented in Ref. [11] to estimate the integral frequency offset in OFDM Worldwide Interoperability for Microwave Access (WiMAX) downlink.

In this letter, we present a new blind frequency offset estimation method based on CP and virtual subcarriers in the CO-OFDM system. It can estimate the fractional part and the integral part of the frequency offset at the same time. Its estimation range is about [−3.5 GHz, 3.5 GHz]. The effect of the integral frequency offset is comprehensively analyzed in CO-OFDM system. We investigate its performance in the additive white Gaussian noise (AWGN) channel and the dispersive channel, respectively. The performance of the proposed method

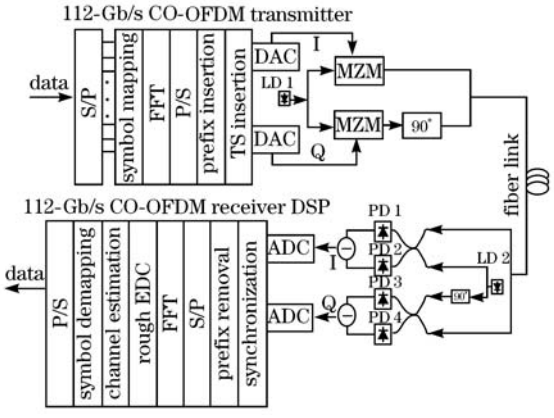


Fig. 1. Block diagram of a 112-Gb/s CO-OFDM system. S/P: serial to parellel; P/S: parellel to serial; LD: laser diode; TS: training symbol; EDC: electronic dispersion compensation; PD: photodiode; ADC: analog-to-digital converter; I: in-phase part; Q: quadrature part.

 

is analyzed through Monte Carlo simulation.

Figure 1 shows the functional block diagram of a representative 112-Gb/s CO-OFDM transmitter and receiver setup[12]. The CO-OFDM system can be divided into five parts: radio frequency (RF) OFDM transmitter, RF-to-optical up converter, fiber link, optical-to-RF down converter, and RF OFDM receiver.

In the RF OFDM transmitter, after serial-to-parallel conversion, the input bits are mapped onto corresponding information symbols and are then carried on the subcarriers of the OFDM symbol. The time domain signal is obtained by using inverse fast Fourier transform (IFFT). After parallel-to-serial conversion, the signal is subsequently added with CP. The training symbols are inserted to estimate the channel impulse response in the receiver. The in-phase part and the quadrature part of the OFDM signal are converted into time waveform through two digital-to-analog converters (DACs), respectively.

In the RF-to-optical up converter, two Mach-Zehnder modulators (MZMs) are used to convert the baseband RF OFDM signal up on the optical carrier wave. In the fiber link, the standard single mode fiber (SSMF) is employed. In the optical-to-RF down converter, a homodyne coherent detection receiver is used to convert the OFDM signal from the optical domain down to the RF domain.

In the RF OFDM receiver, the in-phase part and the quadrature part of the OFDM signal are first sampled with two ADCs, respectively. Synchronization is done before removing the CP. After serial-to-parallel conversion, the OFDM signal is demodulated by discrete Fourier transform (DFT) operation. Because no dispersion compensation fiber (DCF) is used in the fiber link, a rough CD compensation and channel estimation are performed based on training symbols and pilots. Finally, the bits are obtained through symbol demapping and parallel-to-serial conversion.

In the OFDM symbol, not all of subcarriers are used to carry data, for example WiMAX[13]. Meanwhile, the structure of the OFDM symbol in the CO-OFDM system has to be analyzed according to its system characteristics. Owing to the imperfection of the filter, the sideband signal is damaged by the filtering processing. Meanwhile, as frequency offset exists, it can prevent OFDM signals from shifting out of the filter. The direct current (DC) and low frequency are regarded as the virtual subcarriers for the reason that the optical carrier, MZM and other system noises have great influence on these subcarriers. Moreover, frequency offset shifts optical carrier from DC to nearby subcarriers. It is harmful to channel estimation. For the sake of simplicity, we assume the fast Fourier transform (FFT) size is 256. The OFDM symbol frequency domain description in CO-OFDM is illustrated in Fig. 2. In Fig. 2, totally 256 subcarriers are divided into four parts. There are 176 subcarriers for data transmission, 32 subcarriers for pilot tone, 32 subcarriers for guard bands, and 16 subcarriers for DC and low frequency subcarriers in every OFDM symbol. The 176 subcarriers are used to carry the payload data. Because coherent detection in the receiver requires the information of the channel, pilots are inserted in the transmitter. In both edges of the OFDM symbol, 32 subcarriers are used as guard band.

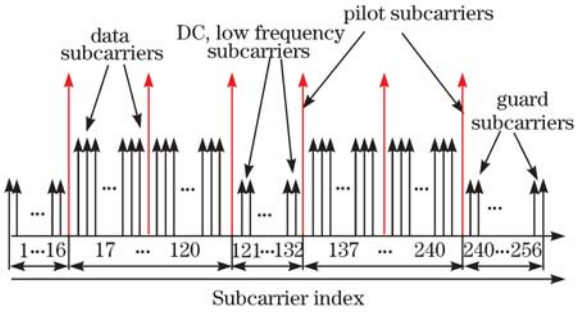


Fig. 2. Structure of OFDM symbol in CO-OFDM system.

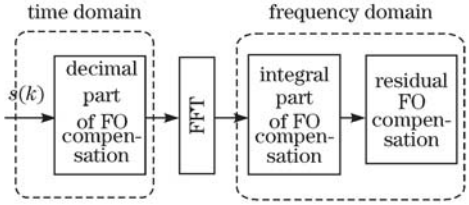


Fig. 3. Conceptual diagram of frequency offset (FO) estimation.

The blind frequency offset estimation method contains three parts: 1) the fractional frequency offset estimation based on CP; 2) the integral frequency offset estimation based on virtual subcarriers; 3) the residual frequency offset compensation based on pilots. In the CO-OFDM receiver, the schematic diagram of frequency offset estimation is depicted in Fig. 3.

The fractional part of the frequency offset destroys the orthogonality between subcarriers. Hence, it must be estimated before FFT[9]. ML estimation of the fractional frequency offset based on CP was introduced in Ref. [10]. In the following analysis, we assume that the channel is nondispersive and the transmission OFDM signal $s(k)$ is only influenced by a complex AWGN. The analysis in the dispersive channel is more complicated. However, the method is also suitable for a dispersive channel.

Assuming that the fractional frequency offset between the transceiver lasers is $\Delta f_{\rm f}$. The sampling frequency offset is $f_{\rm s}$ and the sampling period $T_{\rm s}$ is the inverse of $f_{\rm s}$. $N_{\rm s}$ is the number of subcarriers. The subcarrier spacing $\Delta f$ is the inverse of $N_{\rm s}T_{\rm s}$. OFDM is a special kind of multicarrier modulation. Notice that all the subcarrier experience the same fractional frequency offset $\Delta f_{\rm f}$. The received signal with the effect of $\Delta f_{\rm f}$ and AWGN is

$$r(kT_{\rm s}) = s(kT_{\rm s})\exp(\mathrm{j}2\pi\Delta f_{\rm f}kT_{\rm s}) + n(kT_{\rm s}). \quad (1)$$

It can be expressed as

$$r(k) = s(k)\exp\left(\mathrm{j}2\pi\frac{k\Delta f_{\rm f}}{N\Delta f}\right) + n(k). \quad (2)$$

If $\varepsilon$ denotes $\Delta f_{\rm f}$ as a fraction of the subcarrier spacing $\Delta f$, Eq. (2) is expressed as

$$r(k) = s(k)\exp\left(\mathrm{j}2\pi\frac{k\varepsilon}{N}\right) + n(k). \quad (3)$$

The transmitted signal $s(k)$ is the DFT of the data signal $x(k)$. Therefore, $s(k)$ is a linear combination of independent, identically distributed random variables. If the number of subcarriers is large enough, from the central

limit theorem, we know that $s(k)$ approximates a complex Gaussian process, whose real and imaginary parts are independent. In the receiver, however, $r(k)$ is not white because of the insertion of CP and a correlation between some pairs of samples that are spaced by $N$ samples apart is yielded. Because of its probabilistic structure, it contains information about the frequency offset $\varepsilon$.

Assuming the length of CP is $L$, Fig. 4 shows a complete OFDM symbol with CP. Notice that in one OFDM symbol the samples in the CP and their copies $r(k)$, $k \in [0, \cdots, L-1] \cup [N, \cdots, N+L-1]$ are pairwise correlated,

$$E\{r(k)r^*(k+N)\} = \sigma_s^2 \exp(-\mathrm{j}2\pi\varepsilon). \tag{4}$$

The noise, such as AWGN, has great influence on the performance of this method. To increase the accuracy of this method, $M$ OFDM symbols are employed to perform the fractional frequency offset estimation. Hence, the estimation result is expressed as

$$\phi(\varepsilon) = \sum_{i=0}^{M-1} \sum_{k=0}^{L-1} r_i(k) r_i^*(k+N). \tag{5}$$

We can yield the ML estimation of $\varepsilon$ as

$$\hat{\varepsilon}_{ML} = -\frac{1}{2\pi} \angle \phi(\varepsilon) + n, \tag{6}$$

where $n$ is an integer. A similar frequency offset estimator has been derived under different assumptions[14]. Notice that owing to the periodicity of the exponential function, several values can be acquired. Hence, this method only estimates exactly the fractional frequency offset and that $|\varepsilon| < 1/2$. Thus, $n = 0$.

The estimation for integral frequency offset can be classified into three categories: data-aided methods[15], semi-blind methods[11], and blind methods. The data-aided method estimates the integral frequency offset by sending training symbols, which induces a loss of bandwidth efficiency. We present a new blind integral frequency offset based virtual subcarriers, which are inserted in both sides of the OFDM symbol. Each side contains 16 virtual subcarriers as the guard band. The virtual subcarrier is not only used for integral frequency offset estimation, but also used to prevent OFDM signals from shifting out of the filter as frequency offset exists. Meanwhile, insertion of virtual subcarriers lowers the requirement on the filter. Hence, virtual subcarriers are necessary for the OFDM symbol in the practical CO-OFDM system. In our scheme, virtual subcarriers are employed to estimate the integral frequency offset, without inducing a loss of bandwidth efficiency. In theory, the range of integral frequency offset estimation is about [−3.5 GHz, 3.5 GHz].

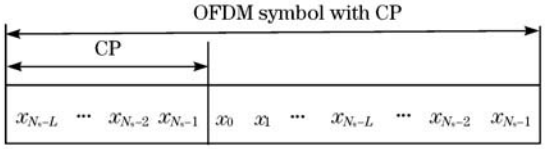


Fig. 4. Structure of OFDM symbol with CP.

Integral frequency offset does not destroy orthogonality between these subcarriers. It has two influences on OFDM signals: firstly, it induces cyclic shift of subcarriers in one OFDM symbol in the frequency domain[16]; secondly, it adds a constant phase shift on all the subcarriers of the same OFDM symbol. Assuming the integral frequency offset is $f_\mathrm{I}$ (normalized by subcarrier spacing $\Delta f$), the received signal is

$$\begin{aligned} r(i,k) &= s(i,k) \exp\left(\mathrm{j}2\pi \frac{f_\mathrm{I}(k+L+(N+L)(i-1))}{N_s}\right) \\ &= s(i,k) \exp\left(\mathrm{j}2\pi \frac{f_\mathrm{I}(k+Li)}{N_s}\right), \end{aligned} \tag{7}$$

where $i$ is the index of OFDM symbol, $k$ is the index of the subcarrier, and $L$ is the length of CP. After DFT demodulation, the received signal is

$$\begin{aligned} Y(i,n) &= \sum_{k=0}^{N_s-1} r(i,k) \exp\left(-\mathrm{j}2\pi \frac{nk}{N_s}\right) \\ &= \sum_{k=0}^{N_s-1} s(i,k) \exp(\mathrm{j}2\pi \frac{f_\mathrm{I}(k+Li)}{N_s}) \exp(-\mathrm{j}2\pi \frac{nk}{N_s}) \\ &= \exp\left(\mathrm{j}2\pi \frac{f_\mathrm{I}Li}{N_s}\right) \sum_{k=0}^{N_s-1} s(i,k) \exp\left(-\mathrm{j}2\pi \frac{k(n-f_\mathrm{I})}{N}\right) \\ &= \exp\left(\mathrm{j}2\pi \frac{f_\mathrm{I}Li}{N_s}\right) S(i, (n-f_\mathrm{I}) \bmod N_s). \end{aligned} \tag{8}$$

The constant phase shift of the $i$th OFDM symbol is $\exp(\mathrm{j}2\pi \frac{f_\mathrm{I}Li}{N})$. Compared with the original signal $S(i,n)$, the received signal $Y(i,n)$ has $f_\mathrm{I}$ shift ($f_\mathrm{I} > 0$: right shift; $f_\mathrm{I} < 0$: left shift). After the insertion of virtual subcarriers, assuming that the number of subcarriers is 256, the transmitted OFDM symbol $S(i)$ is depicted in Fig. 5.

The range of integral frequency offset estimation is about [−3.5 GHz, 3.5 GHz] when 16 virtual subcarriers

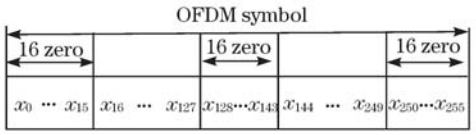


Fig. 5. Structure of OFDM symbol with virtual subcarriers.

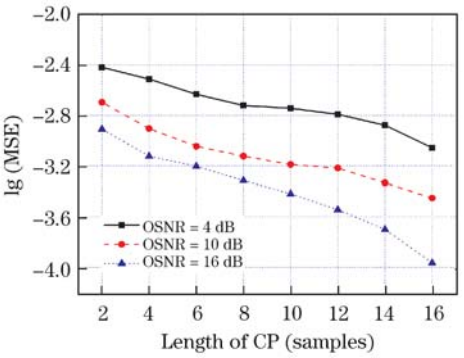


Fig. 6. MSE versus length of CP in the AWGN channel (OSNR = 4, 10, and 16 dB).

are inserted in each side of the OFDM symbol. The power loaded on virtual subcarriers is zero, and these subcarriers are not used to carry data. The process of integral frequency offset estimation based on virtual subcarriers is described as follows.

Step 1: setting a threshold value $V_{\mathrm{D}}$.

Step 2: extracting a block of data, which contains $M$ OFDM symbols, in the OFDM receiver.

Step 3: adding up the amplitude of the same subcarriers in different OFDM symbols together, $AM$ is an $N_{\mathrm{s}} \times 1$ matrix. It is expressed as

$$AM(k) = \sum_{i=0}^{M-1} \mathrm{abs}(Y(i,k)) k \in [1, 2, \cdots, N_{\mathrm{s}}]. \quad (9)$$

Step 4: for $k = 1 : N_{\mathrm{s}}$, if $AM(k) > V_{\mathrm{D}}$, break; $V_{\mathrm{Te}}$ is equal to the current value $k$; this step is used to find the index of the first subcarrier, which is used for carrying data in the left side of the OFDM symbol.

Step 5: $V_{\mathrm{cd}}$ is the first index of subcarrier after virtual subcarriers in the left side of OFDM symbol; in Fig. 6 it is 17; $f_{\mathrm{I}} = V_{\mathrm{Te}} - V_{\mathrm{cd}}$.

The fractional and integral frequency offset methods are not absolutely accurate. There exists a little residual frequency offset. The residual frequency offset induces a phase shift $\Delta\phi$, which is the same to all the subcarriers. The received signal in the $k$th subcarrier is

$$Y(i,k) = S(i,k) \exp(\mathrm{j}\Delta\phi). \quad (10)$$

Pilots are used to estimate the phase shift $\Delta\phi$[17]. $\Delta\phi$ is estimated as

$$\Delta\phi = \angle\left\{\sum_{p=1}^{N_{\mathrm{p}}} [Y(i,k_p) \times S^*(i,k_p)]\right\}, \quad (11)$$

where $N_{\mathrm{p}}$ is the number of pilot subcarriers.

The bit rate is 112 Gb/s. The bits are mapped in a quadrature phase-shift keying (QPSK) constellation. Each subcarrier carries 2 bits to give an optical bandwidth of 56 GHz centered at 193.1 THz. CP is added before each OFDM symbol to combat ISI. We use Monte Carlo simulations to evaluate the performance of the blind frequency offset estimation method in which we consider a CO-OFDM system with 256 subcarriers. We evaluate the performance of our frequency offset estimation method by means of the mean-squared error (MSE). The extinction ratio of the MZM is 30 dB. The ratio of zero padding is 18.75%. The linewidth of laser is 100 kHz. The bandwidth of photodiode is 42 GHz. The Gaussian electrical low pass filter is used after the photodiode, and its bandwidth is 42 GHz .

The simulation platform is VPItransmissionMaker Version 7.6. Simulations are divided into two parts: frequency offset estimation in an AWGN channel, and frequency offset estimation in a dispersive channel.

Simulations are done in a 112-Gb/s back-to-back QPSK CO-OFDM system, which is only affected by AWGN. Performance results for the AWGN channel are shown in Figs. 6, 7, and 8. The MSE of our frequency offset estimation method as a function of the length of CP $L$ is evaluated. Figure 6 shows its performance for optical signal to noise ratio (OSNR) values of 4, 10, and 16 dB when the frequency offset is 1 GHz. Notice that as $L$ increases, the performance of our method shows continuous improvement. Meanwhile, the increase of OSNR is able to improve the performance of our method. When $L$ is longer than 6 (10 dB), the MSE is less than $10^{-3}$. Therefore, our frequency offset scheme works well even if $L$ is short and OSNR is small.

When the frequency offset is 1 GHz, the estimator variances as a function of OSNR for $L = 4$, 8, and 16 are shown in Fig. 7. Notice that as OSNR increases, the performance of our frequency offset estimation method shows continuous improvement. However, performance improvement becomes smaller when the OSNR is larger than 5 dB. This indicates that our method works well in the case of lower OSNR. The performance of our frequency offset estimation method is plotted in Fig. 8 with different frequency offsets. The length of CP is 16. It can be observed that the performance of this method is almost independent of the actual value of the frequency offset. Moreover, the performance is proportional to OSNR.

Simulations are done in a 112-Gb/s QPSK CO-OFDM system, which is affected by both AWGN and CD. The dispersion parameter of fiber is 16 ps/(nm·km). Now, CP has two important roles: estimating the frequency offset and combating the ISI. The CD tolerance of CO-OFDM is proportional to the length of CP. Performance results in the dispersive channel are shown in Figs. 9−12. Firstly, when the OSNR is 10 dB and the frequency offset is 1 GHz, Fig. 9 shows the MSE of our frequency offset estimation method against different CDs with various lengths $L$ of CP. When CD is smaller than 4000 ps/nm,

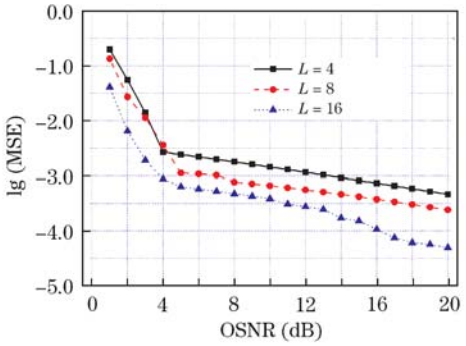


Fig. 7. MSE versus OSNR in the AWGN channel (length of CP $L = 4$, 8, and 16).

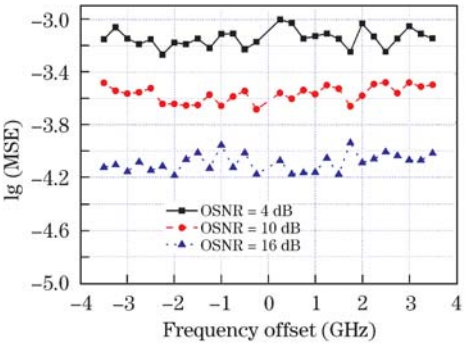


Fig. 8. MSE versus frequency offset in the AWGN channel.

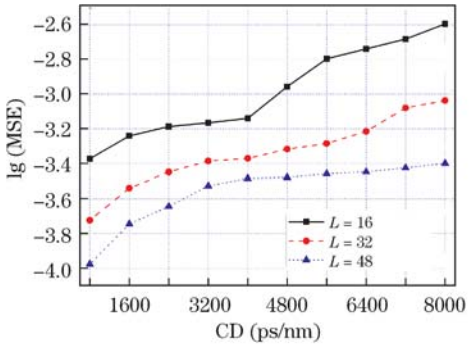


Fig. 9. MSE versus CD ($L$ = 16, 32, and 48).

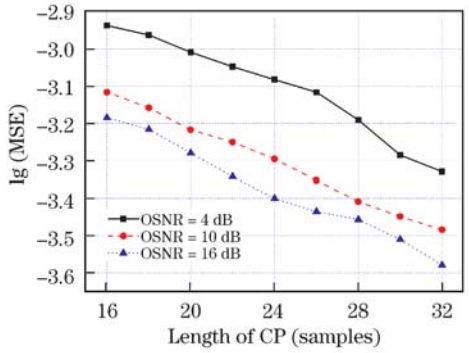


Fig. 10. MSE versus length of CP (CD = 3200 ps/nm; OSNR = 4, 10, and 16 dB).

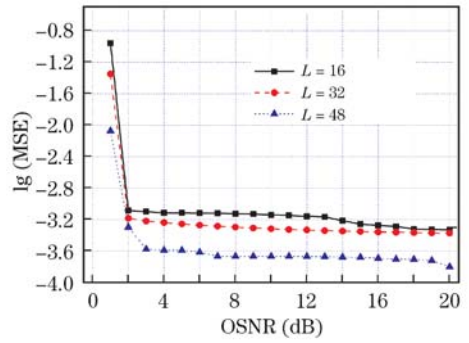


Fig. 11. MSE versus OSNR (CD = 3200 ps/nm; $L$ = 16, 32, and 48).

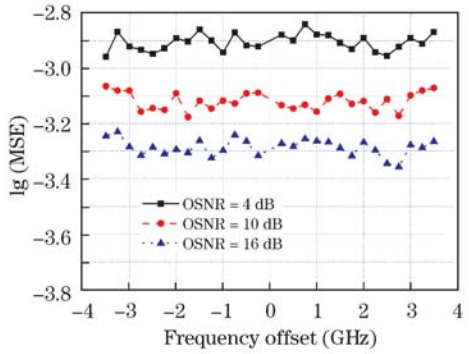


Fig. 12. MSE versus frequency offset (CD = 3200 ps/nm; OSNR = 4, 10, and 16 dB).

the MSE is less than $10^{-3.2}$. It can be found that the performance of our method is inverse proportional to CD and proportional to the length of CP. In the CD tolerance of the CO-OFDM system, it works well. Once CD exceeds the tolerance, the performance significantly degrades. Hence, CD does harm to the performance of our frequency offset estimation method. Second, to observe the effect of CP length more clearly, Fig. 10 shows the MSE against different lengths of CP with various OSNRs when the frequency offset is 1 GHz. The CD is 3200 ps/nm (200 km). As the length of CP increases, the performance of our frequency offset estimation method shows continuous improvement. Meanwhile, its performance is proportional to the OSNR. When the OSNR is 10 dB and the length of CP is 16, the MSE is about $10^{-3.1}$. Compared with the AWGN channel, its performance degrades in the dispersive channel.

Thirdly, when the CD is 3200 ps/nm (200 km) and the frequency offset is 1 GHz, Fig. 11 illustrates the performance of our method against different OSNRs with various lengths of CP. Compared with the AWGN channel, the MSE in the dispersive channel becomes larger, when $L$ is 16. The performance of our method is proportional to the OSNR in the dispersive channel. However, if the OSNR is larger than 4 dB, the improvement of performance becomes slow as the OSNR increases. Finally, to observe the effect of frequency offset more clearly, Fig. 12 indicates the performance of our method against various frequency offsets with different OSNRs when the length of CP is 16. The MSEs of different frequency offsets are almost the same. Hence, the performance of our method is almost independent of the actual value of frequency offset. Besides, the frequency offset of practical laser is in the range [−3.5 GHz, 3.5 GHz]. Therefore, our method is suitable for practical utility in the CO-OFDM system.

In conclusion, a new blind frequency offset estimation method based on the redundancy of both CP and virtual subcarriers is developed for the correction of frequency offset. Our frequency offset estimation method can work well under low OSNR. Even if the OSNR is less than 10 dB and the CP length is very short, the MSE of frequency offset estimation is still less than $10^{-2.5}$. The performance of this method is investigated in an AWGN channel and a dispersive channel, respectively. Simulation results show that it performs well even in the dispersive channel. And it is very robust to CD in the CO-OFDM system. Its range of frequency offset estimation is about [−3.5 GHz, 3.5 GHz]. In addition, it estimates the fraction part and the integral part of the frequency offset at the same time. Meanwhile, our frequency offset estimation method does not need the aid of known data and does not induce the loss of bandwidth effectiveness. Hence, it is very suitable for practical usage in the CO-OFDM system. In the CO-OFDM system, pilots are needed for channel estimation. These pilots can be used by the synchronizer in order to further increase the performance. How to incorporate pilot symbols in such frequency offset estimation method is not clear and awaits further research in the CO-OFDM system.

This work was supported in part by the National Natural Science Foundation of China (No. 60932004), the National "863" Program of China (Nos. 2009AA01Z256, 2009AA01Z253, and 2009AA01A345), and the National "973" Program of China (No. 2007CB310705).

## References


1. T. Ye, F. Liu, and Y. Su, Chin. Opt. Lett. **6,** 398 (2008).
2. J. Gao, Q. Chang, T. Wang, and Y. Su, Chin. Opt. Lett. **6,** 550 (2008).
3. M. Chen, T. Gong, M. Wang, T. Li, and S. Jian, Chin. Opt. Lett. **7,** 683 (2009).
4. W. Shieh, H. Bao, and Y. Tang, Opt. Express **16,** 841 (2008).
5. J. Armstrong, J. Lightwave Technol. **27,** 189 (2009).
6. P. H. Moose, IEEE Trans. Commun. **42,** 2908 (1994).
7. T. M. Schmidl and D. C. Cox, IEEE Trans. Commun. **45,** 1613 (1997).
8. M. J. F.-G. García, O. Edfors, and J. M. Páez-Borrallo, IEEE Trans. Consum. Electron. **47,** 187 (2001).
9. S. Hara and R. Prasad, *Multicarrier Techniques for 4G Mobile Communications* (Artech House, Boston, 2003).
10. J.-J. Van de Beek, M. Sandell, and P. O. Börjesson, IEEE Trans. Signal Process. **45,** 1800 (1997).
11. K.-C. Hung and D. W. Lin, in *Proceedings of IEEE Wireless Communications and Networking Conference* 1959 (2007).
12. W. Shieh, X. Yi, Y. Ma, and Q. Yang, J. Opt. Netw. **7,** 234 (2008).
13. IEEE Standard 802.16-2004, Part 16, "Air interface for fixed broadband wireless access systems" (2004).
14. F. Daffara and O. Adami, in *Proc. Vehic. Technol. Conf.* **2,** 804 (1995).
15. Y. H. Kim, I. Song, S. Yoon, and S. R. Park, IEEE Trans. Vehic. Technol. **50,** 1307 (2001).
16. A. V. Oppenheim, R. W. Schafer, and J. R. Buck, *Discrete-Time Signal Processing* (Prentice Hall, Upper Saddle River, 1999).
17. X. Yi, W. Shieh, and Y. Tang, IEEE Photon. Technol. Lett. **19,** 919 (2007).